Chapter 7
Validation of a General-Purpose Erosion-Sedimentation Model on a Laboratory Experiment

Noémie Gaveau, Carine Lucas, and Frédéric Darboux

Abstract This work aims at modeling transport and sedimentation of particles in a water flow. A new erosion-sedimentation model has been introduced in Nouhou-Bako et al. (J Hydrol X 12:100082, 2021) considering the concentrations of sediment suspended in the fluid or deposited on an exchange layer. Based on conservation laws, it is composed, for each class of particle, of a transport equation on the suspended material, coupled with the exchange between deposited particles and suspended material. A benefit provided by this approach is its ability to replicate other well-known erosion models and thus to model various sedimentation processes and materials. This new model has been implemented into the FullSWOF_1D (Full Shallow Water for Overland Flow in one Dimension) software (Delestre et al. in J Open Source Softw 2:448, 2017) originally designed to solve the Shallow Water equations. The modified software is now able to simulate various erosion situations and was tested against several test cases. In order to check the model even more, we felt important to be able to replicate a laboratory experiment. We chose the sedimentation experiment described in Nouhou-Bako et al. (J Hydrol X 12:100082, 2021) where the transport and deposition of particles by a water flow were studied. The deposited layer and the flux of material at the outlet were measured. Thanks to the physical parameters, and with a calibration limited to settling velocities, we were able to obtain results close to the laboratory measurements. We also propose some clues to improve the results and the model.

N. Gaveau (✉) · C. Lucas
Institut Denis Poisson, UMR 7013, Université d′Orléans, Université de Tours, CNRS, Rue de Chartres, BP 6759, F-45067 Orléans Cedex 2, France
e-mail: Noemie.Gaveau@univ-orleans.fr

C. Lucas
e-mail: Carine.Lucas@univ-orleans.fr

F. Darboux
Université de Lorraine, INRAE, LSE, F-54000 Nancy, France
e-mail: Frederic.Darboux@inrae.fr

Grenoble Alpes, INRAE, ETNA, F-38402 St-Martin-d′Hères, France

P. Gourbesville and G. Caignaert (eds.), *Advances in Hydroinformatics*, Springer Water,
https://doi.org/10.1007/978-981-19-1600-7_7

Keywords Transfer · Equation · Modeling · Flow · Sediments · Experimental results · Shallow water

7.1 Introduction

Erosion and sedimentation processes occur in a wide range of environments: hillslope, river, lake, ocean, etc. [3, 6, 10]. They affect the geomorphology and the ecology of both natural areas and man-made features (such as dams, channels and dykes) [1, 15]. The understanding of these processes is also required to assure water quality and to prevent disasters [7, 12]. A lot of sub-processes are involved and interact (suspension, bedload transport, rolling, saltation, flocculation, dispersion, etc.) [10]. Because experimenting in the field is time-consuming and not always feasible, erosion and sedimentation models are used. Currently, many different models are available depending on the processes and the environment [17].

In [14], we derived a transfer model which replicates several models of the literature, and which can reproduce various physical configurations, such as erosion and sedimentation on hillslope and in rivers. It was shown to reproduce a chemical transport model too, hence its general-purpose. Our model was implemented and coupled to a Shallow Water solver. It was validated against experimental results and analytic solutions.

Recently, we did a laboratory experiment with sediments depositing in a shallow flow [13]. We measured the flux of sediments collected at the outlet and the sediments deposited on the flume bottom. The present article shows that the transfer model coupled to the Shallow Water equations can reproduce the results obtained in this laboratory experiment.

This paper is structured as follows: in Section 7.2, we first detail the model of the transfer equation, and the FullSWOF_1D software that solves the Shallow Water equations and in which the transfer equations are implemented. Then, we describe the laboratory experiment, the configuration of the software to reproduce this experiment and the computed data. In Section 7.3, we show the results obtained with FullSWOF_1D and we compare them with the experimental results. We also discuss how the results could be improved to better fit the experimental configuration. The last section is devoted to the conclusion and perspectives.

7.2 Materials and Methods

7.2.1 A Model for Material Transfer

7.2.1.1 Description of the Model

A unifying transfer model was developed in [14] to simulate transfers of materials by a water flow. One of the goal was to point out that several published equations modelling erosion on hillslope, bedload transport in rivers or chemical transport, can be rewritten under the following unifying formulation:

$$\begin{cases} \frac{\partial(hc_i)}{\partial t} + \frac{\partial(qc_i)}{\partial x} = \frac{1}{ts_i}(G_i(M) - hc_i) + S_i^1 \\ A\frac{\partial M_i}{\partial t} = -\frac{1}{ts_i}(G_i(M) - hc_i) + S_i^2, \end{cases} \tag{7.1}$$

where h [m] and q [m^2 s^{-1}] are the height and the discharge of the fluid, respectively.

This model is based on conservation equations. It expresses the exchanges of materials due to the water flow: the materials enter the flow, they are transported, they can be accreted in an exchange layer and eventually they can be released again. We characterize the materials by their concentrations per unit width in the fluid and in the exchange layer, and also by their size (for sediments) considering several classes of diameters (denoted by the i subscript). In (Eq. 7.1), c_i [kg m^{-2}] and M_i [kg m^{-1}] are the concentrations of the material class i in the fluid and in the exchange layer, respectively, M is the vector of the M_i values, and the S_i^* [kg s^{-1} m^{-1}] are the source terms representing materials from the original soil coming into the system (Fig. 7.1). The parameters G_i (an equilibrium function), ts_i [s] (a relaxation time) and A (a constant coefficient) are chosen depending on the application.

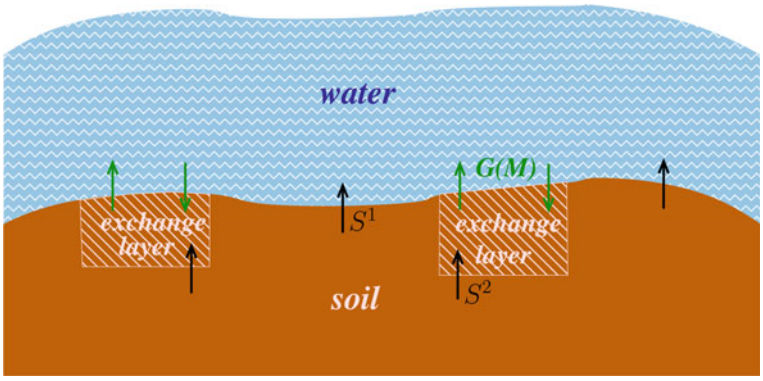

Fig. 7.1 Physical representation of the transfer model (Eq. 7.1) for one class of materials

To complete this model, we need the flow values of height h and flux q at each grid point and each time step. For this purpose, we chose to couple equations (7.1) with the Shallow Water equations, in order to consider applications with thin flows [14]. A consequence of this choice is that the characteristic values of the flow do not depend on the vertical distance. This is a reason why we do not have a vertical variability in the c and M concentrations in the present form.

7.2.1.2 Comparisons With Well-known Models

For different choices of the parameters G_i, ts_i and A of the transfer equations, some models of the literature can be identified. Let us cite three examples. First, the model (Eq. 7.1) can express the Hairsine and Rose model for soil erosion by rainfall on a hillslope [9]. It can also represent bedload transport in rivers as proposed by Lajeunesse et al. [11], and model the proportion of marked tracers in the moving layer and on the bed surface. Finally, this model can also describe chemical transport as modeled by Gao et al. [8], considering dissolved chemical that can move in three different vertically-distributed horizontal layers, with possible transfers between the layers. We refer the reader to [14] for more details on the formulations and the values to choose.

7.2.2 A Software for the Resolution of the Coupled System: Shallow Water and Transfer Model

To solve equations (7.1), we created an independent library implementing a finite volume method in one dimension. The HLL flux was chosen for the numerical scheme at the first order in space, and the MUSCL reconstruction was used to get the second order in space. Details of the numerical method can be found in [14].

This library was coupled to the FullSWOF_1D software (version 2.00.00). It is an object-oriented code written in C++, designed to solve the Shallow Water equations with a finite volume method [5]. The transfer equations are solved at each time step, after updating the flow variables (splitting method). The coupled software was validated against several benchmarks and test cases: First, an approximation of an analytic solution for two classes of particles distributed in the flow and in the exchange layer was found. This solution enabled us to check the proper functioning of the transfer library. Then, the software was confronted to the configuration of Lajeunesse *et al.* for the bedload transport. It is also a benchmark as we know its analytic solution. With this software, we were also able to reproduce the experimental results of Gao *et al.* for the chemical transport, and to improve the results of Hairsine and Rose.

When implementing the transfer equations, we also studied the numerical conservation of mass, comparing the input material mass to the deposited and output masses.

We performed a study for various space steps and flow conditions: the total mass is conserved along the run.

7.2.3 Laboratory Experiment

7.2.3.1 Experimental Data

Experimental data were collected in a laboratory flume. The flume was 1.9 m long and 0.5 m wide. It was set horizontally. It had a rough bottom made of glued sand grains (except for the outlet section). Water was supplied at the closed end at a rate of 73.5 L min^{-1}. A 98-cm section allowed for flow stabilization. It was followed by a sediment feeder that supplied dried sediments from above the whole flume width at a rate of 0.23 ± 0.02 g min^{-1} cm^{-1}. The dried sediment had a bulk density of 2.3 g cm^{-1} and a diameter of 100–200 μm, leading to estimated settling velocities ranging from 5 to 16 mm s^{-1} (based on [4]). The experimental section started 9 cm after the sediment feeder and was 53 cm long. In the experimental section, the flow depth was equal to 26 mm, as measured with a comparator. The experimental section was followed by a 30-cm-long outlet section.

The experimental conditions were chosen so that deposited sediments were not susceptible to be mobilized again. Preliminary testing confirmed that no detachment from the bed floor occurred. After setting the flow, the feeder was switched on for 7 mins. After switching off the feeder, the experiment was kept going for 3 more minutes to allow all sediments to either deposit or exit the flume.

Sediment flux and deposited particles were measured. The sediments were collected at the outlet by placing a 50-μm sieve in the flow for one-minute intervals. The collected sediments were then dried in an oven before being weighted. The sediment flux was estimated as the mass of sediment during the one-minute duration. Deposited sediments were measured at the end of each experimental run by collecting strips of sediments of a few centimeters wide from the flume bottom. Sediments were then air-dried and weighted.

This experiment was replicated three times, see [13] for more details.

7.2.3.2 Parameters of the Simulation

At this stage, a key point must be underlined. In the transfer model (Eq. 7.1), the sediments concentration in the fluid is defined as uniform over the whole water height at all times and locations (and especially at the location where the sediments are added). In the experiments, the particles are fed at the water surface by the feeder, and then the particles start to settle through the water column according to their settling velocity and the flow properties. Hence, by design, the particles in the experiment get transported along the flow direction before the first ones reach the bottom. This led to a lag between the feeding location and the beginning of the

deposit. In the simulation, there is no such a lag because there are particles close to the bottom from the very beginning. As a consequence, a shift in the numerical results will be introduced to reproduce the experimental lag. We discuss this point in the result section.

In order to run the coupled FullSWOF_1D software solving Shallow Water equations and the transfer model (Eq. 7.1), a number of parameters must be set. Note that, in a first step, the physical parameters are not fitted to better match the experimental results, but are directly measured or taken from the literature and used as they are. The main point in the parametrization of FullSWOF_1D concerns the sediments: the sedimentation velocities have to be specified. They were estimated beforehand for different sizes of sediment. Initially, there are no sediment in the water, nor in the exchange layer. The quantity of sediment entering into the system is controlled as explained in the description of the experimental device.

Regarding the flow, in order to match laboratory conditions, we impose the water height at the inlet and at the outlet. Throughout the domain, the water height is initially set to 26 mm and water velocity to 0.09 m s^{-1}. The experimental water height and discharge are attained: the solution of the Shallow Water equations, initialized to the measured values, do not evolve in time.

The parameters of the equations (7.1) are chosen to model the Hairsine and Rose configuration in the above experimental conditions: the constant A is equal to 1, the equilibrium function G_i is the zero function as the deposited particles cannot move again, and the ts_i values are given by $ts_i = h/v_i$ where v_i is the settling velocity of the i^{th} class of sediments.

7.2.4 Computation Outputs

Coupled with equations (7.1), the FullSWOF_1D software outputs both hydrodynamic and erosion-related variables: in addition to the water height and velocity computed thanks to the Shallow Water equations, the software also gives, for each class of particles, their concentrations in the water and in the deposited layer in the domain. We keep in check the amount of sediment entering and exiting the domain. We are also able to calculate the mass of sediments in suspension and deposited at any point of the domain.

7.3 Results and Discussion

7.3.1 Comparison of Simulation and Laboratory Results

As explained in the previous section, our goal is to confront the numerical simulations to the experimental results. At the end of the experiment, there are no sediments left

in the water. They either exited the domain or were deposited on the flume bottom. In this section we compare, on the one hand, the spatial profile of the deposited sediments in the domain at the end of the experiment, and, on the other hand, the temporal profile of the flux of sediments exiting the domain during the experiment. Let us recall that, as the particles are experimentally fed at the water surface (which causes a lag before sedimentation occurs), the numerical results need to be shifted.

To get the first results, we restrain ourselves to the estimated range of settling velocities (between 5 and 16 mm s^{-1}). For the second results, this constraint is relaxed and we consider a wider range of velocities.

7.3.1.1 Strict Range of Velocities

As stated before, estimated settling velocities range from 5 to 16 mm s^{-1} for a size range of 100-200 μm. As we do not know the sediment size distribution within this range, those velocities can be distributed in various ways. To find which distribution better accounts for both the spatial and the temporal profiles, we performed preliminary tests with a uniform repartition, with a Gaussian repartition, and by weighting the proportion of particles having the minimum and maximum velocities. We concluded that the best fit was achieved when a 1–to–9 ratio of the min. and max. velocities was used (i.e., setting nine tenth of the input mass of sediments with a velocity of 16 mm s^{-1} and one tenth at 5 mm s^{-1}). This is the configuration used to get the results of Figs. 7.2 and 7.3.

On Fig. 7.2, we plotted the deposited sediments as a function of space, after the 10 minutes run for the three experiments and for the numerical simulation with the FullSWOF_1D software. Laboratory results show first a limited deposit of sediments, followed by a peak (around 10–15 cm), and then a slow decrease of concentration. The initial low deposit followed by a peak is due to the particles being fed at the water surface: before being deposited, particles needed to settle through the water layer, while being transported toward the flume end. This gives rise to a lag distance between the sediment feeder location and the peak position. Because the transfer model assumes the sediments to be uniformly distributed on the water height as soon as they are added to the flow, by design, we are not able to reproduce numerically the behavior of the sediment deposit in the first 15 cm of the domain, and we need to shift our graph in order to compensate for that lag. With this shift accounted for, the general decrease of the experimental curve is fairly represented by the numerical simulation, especially toward the end of the domain, although the FullSWOF_1D curve would need to be a bit steeper in order to better match the experimental data between 15 and 25 cm. Despite those differences, the overall mass of sediment deposited in the domain at the end of the simulation are on par with the experimental one, with 73 g deposited by FullSWOF_1D, and 70 g in average on the three experiments.

On Fig. 7.3, we represented the mass of sediment exiting the domain during the duration of the experiment. After the first minute, the flux of sediment is almost constant up to the 7^{th} minute. After the 7^{th} minute, it abruptly decreases (at the moment the particle influx is stopped). Although we obtain slightly lower values

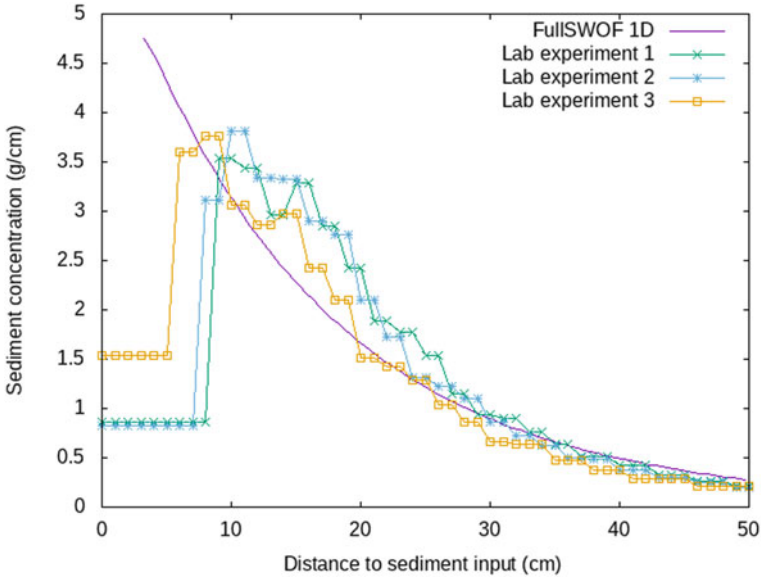

Fig. 7.2 Sediment deposit on the domain at the end of the experimental runs, and for a 1-to-9 ratio of sediment velocities equal to 5 and 16 mm s^{-1}, respectively, with a 3 cm shift

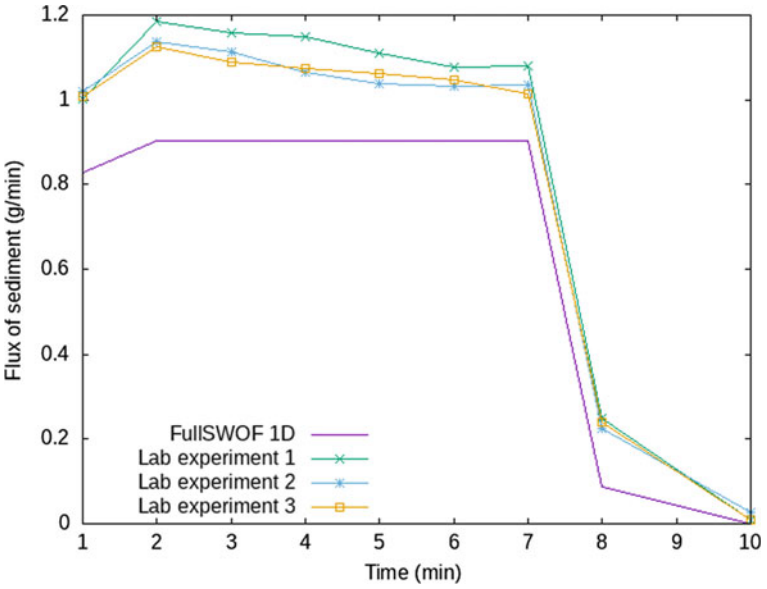

Fig. 7.3 Sediment flux at the outlet in function of time for the experimental runs, and for a 1-to-9 ratio of sediment velocities 5 and 16 mm s^{-1}, respectively

using FullSWOF_1D, the shape of the graph is similar to the one obtained in the laboratory. This difference is consistent with the greater mass of sediments deposited inside the domain by the model (i.e., 73 g instead of 70 g).

7.3.1.2 Extended Range of Velocities

Though the previous results are satisfying, one might wonder if they could be improved by relaxing our constraints. Specifically, the settling velocities were not measured, but estimated based on the literature. In the following, we allow for a broader range of sedimentation velocities, but using a single velocity for the whole range of sediment sizes (the only other free parameter is the shift). We thus simulate the sediment deposit and the sediment output flux for velocities ranging from 10 to 30 mm s^{-1} (Figs. 7.4 and 7.5). In order to not overcrowd the figures, the simulation results are compared to the mean value of the three laboratory experiments.

The profiles of sediment deposit and output flux for the different velocities are consistent with the expected behavior: as the sedimentation velocity increases, more sediments are deposited at the beginning of the domain, leading to a steeper curve in Fig. 7.4, and fewer sediments reach the end of the domain, leading to a lower constant flux at the outlet on Fig. 7.5.

Those two figures clearly illustrate the need to adjust the velocity distributions in the input mix of sediments. Indeed, the best match on Fig. 7.4 seems to be with a

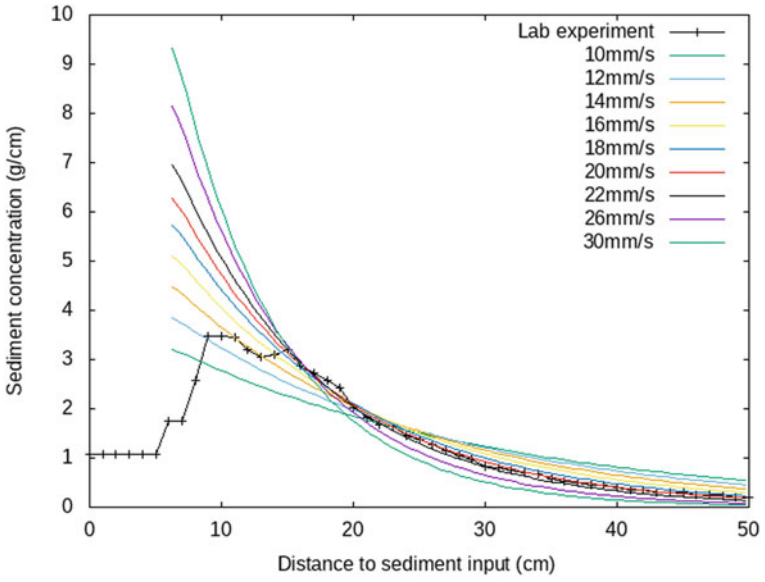

Fig. 7.4 Sediment deposit on the domain at the end of the experimental runs after 10 minutes, and for different simulated sedimentation velocities, with a 6 cm shift

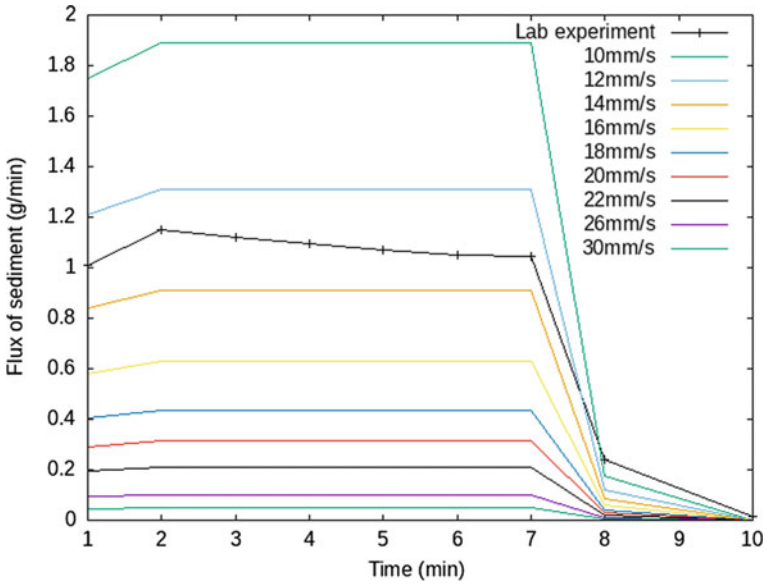

Fig. 7.5 Sediment output flux in function of time for the experimental runs and for different sedimentation velocities

velocity of about 22 mm s^{-1}, while, on Fig. 7.5, one would prefer a lower velocity of 13 mm s^{-1}. To improve the numerical results, a blend of velocities could be used in order to better fit the general shape and values of both figures.

7.3.2 Possible Improvements of the Model

The choice of representing the sediment concentration as a function of only the horizontal distance, not the vertical distance, shows some limitations and induces a need for adjustments. Indeed, and as stated before, the sediment concentration in the laboratory experiment is not homogeneous across the water height. The consequence of this difference is very obvious on the figures: the simulated sediment deposition starts right at the left boundary of the domain, while more distance is necessary on the laboratory experiment for the deposit to peak. In order to properly compare the results, we thus had to either shift the simulation graph, or cut out the beginning of the laboratory curves. This shift distance is freely chosen, but yields an acceptable relative error as long as it stays within the boundaries of a few centimeters.

To improve the model and represent the peak of sediment deposit (and not to have to shift the graph), one could impose a vertical dependency of c and M. If the vertical profile of the concentrations in sediments is *a priori* known, one can recover the vertical variability from the mean value of the concentrations. Another

approach would be to use a different flow model altogether, either based on the Navier-Stokes equations [18] such as in the Gerris software [16], or considering a multi-layer Shallow Water model [2]. In such a way, the water height and velocity of the fluid could vary with the vertical distance; then, modifying model (Eq. 7.1), the sediment concentration could also depend on the vertical distance, and better fit to the experimental design.

7.4 Conclusion and Perspectives

Using the model of the transfer equations and the FullSWOF_1D software, we were able to reproduce the results obtained in the experiments. Laboratory sediment deposit and output were matched by the numerical simulation with almost no calibration, using only the parameters of the experiments. However, the use of a one-layer Shallow Water model leads to a need for adjustments to better fit the results. This is due to the heterogeneity of the sediments along the z-axis in the experiments, a variable that is not accounted for in the present simulations.

To pursue and improve on this work, one could introduce a vertical dependency on the water concentration of sediments, or use another model than Shallow Water to simulate the hydrodynamic variables. More test cases would also allow us to have a better understanding of the capacities and limitations of the model when used to predict natural events.

Acknowledgments The authors thank Lionel Cottenot and Pierre Courtemanche for their technical skills in building and running the experiments. The project "Multiparticular transfer by overland flow" of CNRS-INSU 2016 TelluS-INSMI-MI funded part of the experiments.

References

1. Arnaud-Fassetta G (2003) River channel changes in the Rhone Delta (France) since the end of the Little Ice Age: geomorphological adjustment to hydroclimatic change and natural resource management. Catena 51(2):141–172
2. Audusse E, Bristeau MO, Perthame B, Sainte-Marie J (2011) A multilayer Saint-Venant system with mass exchanges for shallow water flows. Derivation and numerical validation. M2AN Math Model Numer Anal 45:169–200
3. Bartley R, Poesen J, Wilkinson S, Vanmaercke M (2020) A review of the magnitude and response times for sediment yield reductions following the rehabilitation of gullied landscape. Earth Surf Process Landforms 45(13):3250–3279
4. Cheng NS (1997) Simplified settling velocity formula for sediment particle. J Hydraulic Eng 123(2):149–152
5. Delestre O, Lucas C, Darboux F, Ksinant P-A, Darboux F, Laguerre C, Vo TNT, James F, Cordier S (2017) FullSWOF: full shallow-water equations for overland flow. J Open Source Softw 2(20):448
6. East AE, Pess GP, Bountry JA, Magirl CS, Ritchie AC, Logan JB, Randle TJ, Mastin MC, Minear JT, Duda JJ, Liermann MC, McHenry ML, Beechie TJ, Shafroth PB (2015) Large-scale

dam removal on the Elwha River, Washington, USA: river channel and floodplain geomorphic change. Geomorphology 246:687–708
7. Fu BH, Merritt WS, Croke BFW, Weber TR, Jakeman A. J. (2019). A review of catchment-scale water quality and erosion models and a synthesis of future prospects. Environ Model Softw 114:75–97
8. Gao B, Walter MT, Steenhuis TS, Hogarth WL, Parlange J-Y (2004) Rainfall induced chemical transport from soil to runoff: Theory and experiments. J Hydrol 295:291–304
9. Hairsine PB, Beuselinck L, Sander GC (2002) Sediment transport through an area of net deposition. Water Resourc Res 38(6):22.1–22.7
10. Julien P. Y. (2010). *Erosion and Sedimentation.* Cambridge University Press. 2nd edition.
11. Lajeunesse E, Devauchelle O, Houssais M, Seizilles G (2013) Tracer dispersion in bedload transport. Adv Geosci 37:1–6
12. Mouri G, Shiiba M, Hori T, Oki T (2011) Modeling reservoir sedimentation associated with an extreme flood and sediment flux in a mountainous granitoid catchment Japan. Geomorphology 125(2):263–270
13. Nouhou-Bako A, Cottenot L, Courtemanche P, Lucas C, James F, Darboux F (2022) Impacts of raindrops increase particle sedimentation in a sheet flow. Earth Surf Process Landforms 47(5):1322–1332
14. Nouhou-Bako A, Lucas C, Darboux F, James F, Gaveau N (2021) A unifying model for soil erosion, river bedload and chemical transport. J Hydrol X 12:100082
15. Ock G, Gaeuman D, McSloy J, Kondolf GM (2015) Ecological functions of restored gravel bars, the Trinity River California. Ecol Eng 83:49–60
16. Popinet S (2009) An accurate adaptive solver for surface-tension-driven interfacial flows. J Comput Phys 228:5838–5866
17. Reed S, Koren V, Smith M, Zhang Z, Moreda F, Seo DJ (2004) Overall distributed model intercomparison project results. J Hydrol 298(1–4):27–60
18. Stokes GG (1851) On the effect of internal friction of fluids on the motion of pendulums. Trans Cambridge Phil Soc 9:80–85